

MBE HgCdTe :A Challenge to the Realization of Third Generation Infrared FPAs

He Li[†], Chen Lu, Wu Jun, Wu Yan, Wang Yuanzhang, Yu Meifang, Yang Jianrong,
Ding Ruijun, Hu Xiaoning, Li Yanjin, and Zhang Qinyao

(Research Center for Advanced Materials and Devices, Shanghai Institute of Technical Physics,
Chinese Academy of Sciences, Shanghai 200083, China)

Abstract : Some results on the molecular-beam epitaxial growth of HgCdTe focusing on the requirements of the 3rd generation infrared focal plane arrays are described. Good uniformity is observed over 75mm HgCdTe epilayers, and the deviation in cutoff wavelength is within 0.1 μ m at 80K. A variety of surface defects are observed and the formation mechanism is discussed. The average density of surface defects in 75mm HgCdTe epilayers is found to be less than 300cm⁻². It is found that the surface sticking coefficient of As during HgCdTe growth is very low and is sensitive to growth temperature, being only $\sim 1 \times 10^{-4}$ at 170 . The activation energy of As in HgCdTe was determined to be 19.5meV, which decreases as $(N_a - N_d)^{1/3}$ with a slope of 3.1×10^{-5} meV · cm. The diffusion coefficients of As in HgCdTe of $1.0 \pm 0.9 \times 10^{-16}$, $8 \pm 3 \times 10^{-15}$, and $1.5 \pm 0.9 \times 10^{-13}$ cm²/s are obtained at temperatures of 240, 380, and 440 , respectively under Hg-saturated pressure. The MBE-grown HgCdTe is incorporated into FPA fabrications, and the preliminary results are presented.

Key words : MBE; HgCdTe; infrared focal plane arrays

EEACC : 2520

CLC number : TN304.54

Document code : A

Article ID : 0253-4177(2006)03-0381-07

1 Introduction

Third generation infrared imaging systems require Hg_{1-x}Cd_xTe-based infrared focal plane arrays (IRFPAs) with increased formats and multi-color sensing capabilities^[1]. The capability of *in situ* formation of pn junctions^[2], hetero-epitaxial growth on large-area lattice-mismatched substrates of GaAs, Ge^[3], and Si^[4] thermally-matched with readout chips, and the ability to control surface morphology are becoming the most important issues in pushing the technique of molecular-beam epitaxy (MBE) of HgCdTe to maturity, and have been extensively studied by many groups worldwide.

The major challenges are the growth of high-quality epilayers on highly lattice-mismatched and thermally-mismatched foreign substrates, surface morphology, and extrinsic p-type doping with As.

Surface defects as well as dislocations in the HgCdTe are known as "device killers"^[5,6], which seriously degrade device performance. Because of the very low sticking coefficient of Hg, the nucleation of surface defects is a sensitive function of the growth conditions employed. In order to obtain material with a lower dislocation density, the lattice-matched Cd_{0.96}Zn_{0.04}Te is commonly employed as a substrate for HgCdTe epitaxy. However, Cd_{0.96}Zn_{0.04}Te suffers from the problems of relatively small area and poor thermal compatibility with silicon readout chips, which results in the failure of FPAs during temperature cycling.

It has been recognized that the difficulties in the As-doping of MBE-grown HgCdTe mainly come from the amphoteric behavior of As due to the Te-rich growth mode and the low-temperature growth condition as required by the low surface-sticking coefficient (SSC) of As, which further complicates the understanding of the primary pos-

[†] Corresponding author. Email: lihe@mail.sitp.ac.cn

sible modes of As incorporation.

This paper describes some of our results obtained at the Center for Advanced Materials and Devices (CAMD) in an attempt to address the challenges mentioned above.

2 Growth on GaAs and Si substrates

The growth was performed in a Riber 32P system with sources of Zn, CdTe, Te, Hg, As₄, and In. We employed 75mm GaAs (211) B and Si (211) wafers as substrates. To reduce the lattice-mismatching between the HgCdTe and the substrates, a buffer layer composed of either ZnTe/ CdTe or CdTe was grown prior to the HgCdTe nucleation. The thickness of the buffer layer was in the range from 3 to 12 μm . A spectroscopic ellipsometer (SE) capable of utilizing 44 different wavelengths in the range of 410 ~ 761nm (J. A. Woollam Inc.) was attached to the MBE chamber at an angle of approximately 70° for in situ real-time monitoring of composition variation. The x value and the thickness were evaluated by IR transmission measurements, which were carried out by using a Fourier transformer spectrometer (BRO-RAD STF-65A). To avoid the uncertainties in determining the x value and the thickness resulting from the multilayer interference in transmission curves, a computer simulation based on a simple model of the multilayer interference was performed in an attempt to unambiguously determine these parameters^[7].

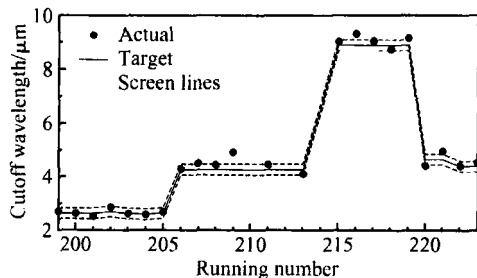


Fig. 1 Controllability in cutoff wavelength

The composition uniformity is a major issue of concern in developing HgCdTe MBE technology. By refining the processes of both flux measurements and the amount of charging material in crucibles, a significant improvement in composition reproducibility was achieved. For long wave-

length (LW) applications (a mean x value of 0.229), a standard deviation (STDDEV) in x of less than 0.0017 was obtained in a run-to-run base. As shown in Fig. 1, a yield of cut-off wavelength of 73 % was obtained as screened by a deviation of less than 0.2 μm from the targets. The HgCdTe epilayers showed good lateral uniformity in both composition and thickness. Figure 2 shows an example of composition or cutoff uniformity for a 75mm HgCdTe wafer grown on Si. The maximum deviation in cutoff wavelength at 80 K is less 0.1 μm over the central area of a diameter of 70mm, satisfying the requirements for FPA fabrication.

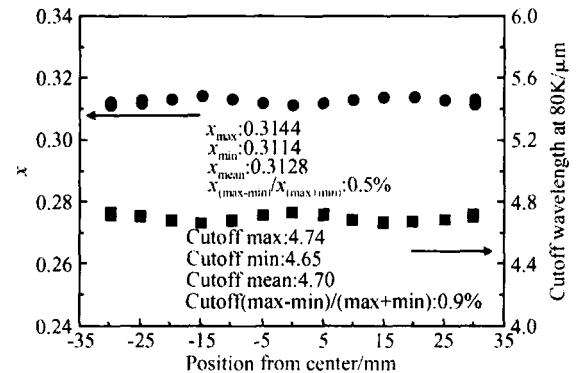


Fig. 2 Composition and cutoff wavelength uniformity for a 75mm HgCdTe wafer on Si

To overcome the problem of the large lattice-mismatch (19.3 %) between HgCdTe and Si, a procedure consisting of As passivation, low-temperature nucleation of ZnTe followed by high-temperature annealing, and the subsequent growth of ZnTe and CdTe at normal temperatures were employed on Si substrates. A high density of dislocations was generally exhibited in the as-grown HgCdTe, with typical EPD values at the surfaces of $9 \sim 20 \times 10^6 \text{cm}^{-2}$. In order to reduce the dislocation density, an in situ high-temperature annealing procedure was employed. The samples were capped with ZnTe or ZnSe at the growth end and annealed inside the growth chamber at 350 ~ 450 for 10 ~ 20min. The EPD value could be effectively reduced to typically $(2 \sim 4) \times 10^6 \text{cm}^{-2}$ for LW samples.

For growth on highly lattice-mismatched substrates, twinning is likely to occur in the epilayers. X-ray high-resolution diffraction (XRD) (Philips X'Pert Pro MRD) analysis showed that the HgCdTe was in the [211] orientation, and no

twinning-related [133] peak was found. It was found that the formation of (133) twins was closely related to the nucleation temperature for the first layer of ZnTe as well as the proper condition for high-temperature growth. The full width at half maximum (FWHM) values for HgCdTe epilayers grown on GaAs and Si were typically 60 ~ 80 . An example of the FWHM mapping of diffraction curves of HgCdTe grown on Si is shown in Fig. 3.

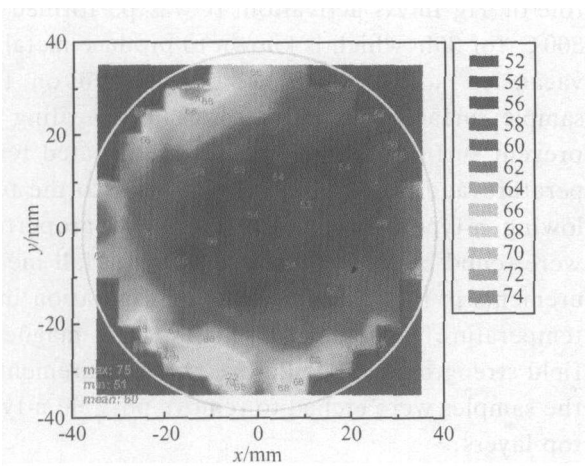


Fig.3 FWHM mapping of XRD on 75mm HgCdTe grown on Si

3 Surface defects

The surface defects in the pixels of FPAs can seriously degrade the performance of the devices. Because of the very low sticking coefficient of Hg , the nucleation of surface defects is a sensitive function of the growth conditions employed. In

order to minimize the density of the surface defects ,the origin of defect nucleation as well as its relation with the growth conditions should be clarified.

The features of various surface defects on HgCdTe epilayers grown under different conditions were studied by using scanning electron microscopy (SEM),energy dispersive X-ray fluorescence spectroscopy (EDX),and atomic force microscopy (AFM). The EDX analysis was performed by using standardless ZAF corrections (atomic number ,absorption and fluorescence coefficients) for qualification.

As shown in Fig. 4 ,various kinds of surface defects were observed on the HgCdTe surfaces. Some of these defects were voids ,some were hillocks ,and some were mixture of voids and hillocks. The origin of these defects is either substrate-related ,growth-related or both substrate- and growth-related. Figures 4 (a) ~ (c) show substrate related defects (type 3) ;(d) shows voids related to Hg-deficiency (type 2) ;(e) ~ (f) show the voids when Hg is further deficient (type 1) ;(g) shows defects related to Hg enrichment (type 4),and (h) shows the void sometimes observed when the growth temperature was lowered from the optimal condition by ~2 (type 5). For FPA applications ,obviously type 1 ~ 3 defects are more problematic because they are large in size and may penetrate deep into the film. Even one such defect may completely kill the pixel. By efforts in substrate preparation and control of growth conditions ,the density of surface defects of HgCdTe has been reduced to less than 300cm⁻².

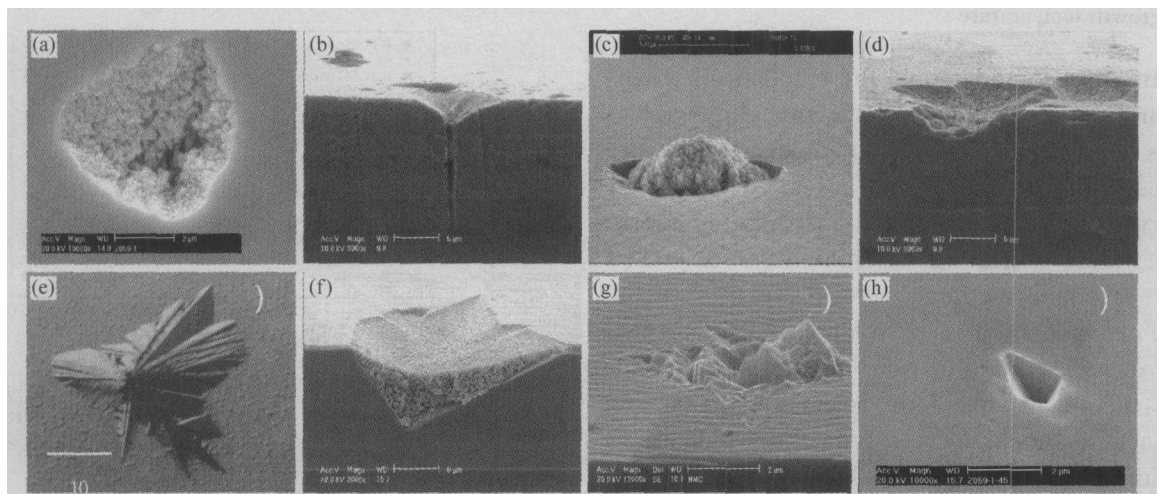


Fig.4 SEM and Normaski (e) micrographs of surface defects

4 As incorporation

To understand the sticking behavior of As atom and its relation to the presence of Hg, the SSC of As during HgCdTe growth was measured as shown in Fig. 5. As compared with CdTe, the As sticking in HgCdTe shows surprisingly different behavior, decreasing much more rapidly with increasing temperature by more than an order of magnitude within a temperature increment of only 10 °C. The temperature sensitive behavior of As sticking suggests that the ability to control growth temperature is critical in terms of doping stability as well. A deviation in growth temperature of 1 °C would cause a variation of more than 10 % in doping concentration when growing in the 160 ~ 170 °C range. As shown in Fig. 5, the fact that the SSC of As in HgCdTe is much lower than that in CdTe at the temperatures higher than 160 °C implies that it may have some correlation with the sticking behavior of Hg.

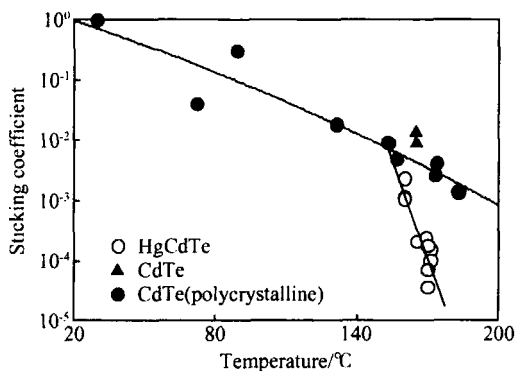


Fig. 5 SSC of As in CdTe and HgCdTe as functions of growth temperature

In order to understand the behavior of As incorporation in the epilayers, the annealing experiments were carried out either under Hg pressure in closed quartz ampoules in a dual-zone oven, or in a vacuum environment at different temperatures. Before annealing, the samples were etched with a bromine methanol solution to remove the CdTe cap layers. The experiments were performed with different combinations of three basic anneals: the n-type anneal, the activation anneal, and the vacuum-anneal. Here n-type anneal means an annealing at 240 °C for 48h under Hg-saturated pressure to annihilate the metallic vacancies created either during the growth or during other annealing processes. All

the annealing experiments in this study were terminated with an n-type anneal. Some samples were pre-annealed with this procedure prior to the other anneals. The activation anneal or p-type anneal refers the annealing in a temperature range of 285 to 440 °C for 0.5 to 30h at different Hg pressures. This process also creates metallic vacancies. The vacuum-anneal is performed in vacuum without participation of the out-coming Hg and is aimed to understand the role of Hg in As activation. It was performed at 360 °C for 30h, which is known to produce metallic vacancies^[8]. ZnS layers were deposited on the sample surfaces before the vacuum-annealing to prevent surface degradation at the elevated temperature, and they were removed prior to the following n-type anneals. The electrical properties were found by temperature-dependent Hall measurements in the Van der Pauw configuration in a temperature range of 300 ~ 12 K at a magnetic field strength of 0.2 T. Before the measurements, the samples were etched to remove possible n-type top layers.

The temperature-dependent Hall measurements for undoped as-grown samples grown at 170 °C showed a compensated n-type characteristic. Figure 6 shows the hole concentration as a function of the doping level of the epilayers annealed at different conditions for activation. The general trend in As activation is consistent with those reported^[9], the electrical activation approaches 100 % when the doping level is low, and saturates or drops as the doping level increases beyond $\sim 1 \times 10^{18} \text{ cm}^{-3}$.

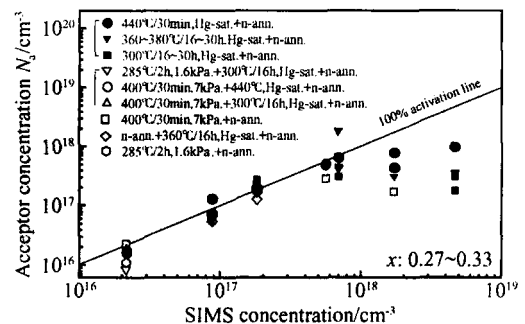


Fig. 6 Hole concentration as a function of the doping level of the epilayers annealed at different conditions for activation

Berding *et al.*^[10] proposed that the As atoms incorporate primarily as a neutral complex com-

posed of As occupying a metallic sublattice and a metallic vacancy, ($A_{SM}-V_M$), bound to a metallic vacancy acceptor, and as isolated A_{SM} donors. It is suspected that in the as-grown samples, the As atoms were possibly incorporated as donors surrounded by additional metallic vacancies which are possibly associated with a large lattice distortion created by the As. The As donors could be isolated atoms in the metallic sublattices or some other structural defects like As_4 tetramers and clusters. Both ambient Hg and metallic vacancies are commonly believed to take important roles in the site transfer process for As atoms into the Te-sublattices. It was predicted that during the activation annealing, the Hg atoms from the ambient would first replace the As atoms occupying the metallic sublattices, and that these As atoms would then replace Te atoms at the Te sites and become the acceptors^[11], or first Te atoms would transfer to the metallic vacancies, generating antisite defects paired with metallic vacancies, followed by the transfer of As atoms to the evacuated Te-sublattices to form acceptors^[10]. To verify the effects of Hg on the activation, vacuum anneals were performed on some of the samples (doping levels from 1×10^{17} to $2 \times 10^{17} \text{ cm}^{-3}$). The Hall measurements on those samples (not shown in the figure) indicate that only 2% ~ 4% of the As atoms were converted to acceptors without the help of Hg, confirming the effect of Hg in As activation. In an attempt to understand the roles of metallic vacancies, two kinds of opposite pre-anneals were employed. One was an n-type pre-anneal to annihilate the metallic vacancies created either during growth or by As incorporation as mentioned above, and the other one was a p-type pre-anneal at 285 and 400 °C and Hg partial pressures of 1600 and 7000 Pa (Te-saturated limit), respectively, to introduce more metallic vacancies at the beginning. The pre-treated samples were then subsequently annealed at 300, 360, and 440 °C under Hg-saturated pressure. As shown in Fig. 6, the results did not cause any remarkable change in As activation compared to those without the pre-treatment. The result can be explained by the fact that the metallic vacancies were also created during the activation anneals regardless of the initial concentration of the metallic vacancies. Another attempt was to vary the Hg partial pressure during the activation an-

neals. As shown in Fig. 6, a certain amount of As could be activated during low temperature anneals at 285 °C even under a Hg partial pressure of 1.6 kPa. For samples annealed at 400 °C at the Te-saturated limit, a noticeable reduction in activation was observed for highly doped samples ($> 1 \times 10^{18} \text{ cm}^{-3}$) as compared with those annealed under the Hg-saturation. The activation energy E_a of As acceptors in HgCdTe was determined by curve-fitting the temperature-dependent Hall concentration with the theoretical model considering a single level of acceptors^[12]. The activation energy for the isolated acceptors, E_0 , was found to be 19.5 meV, which decreased with increasing $(N_a - N_d)^{1/3}$ in a slope of $3.1 \times 10^{-5} \text{ meV} \cdot \text{cm}^{-1/3}$.

The As diffusion in HgCdTe was experimentally investigated using SIMS depth profile analysis on the samples annealed at different conditions. As described above, thermal annealing under Hg pressure is an effective way to electrically activate As. However, the thermal process will destroy the interfaces of a multilayered structure obtained by low temperature growth, the major advantage of MBE. It also causes the As to diffuse, degrading the pn junctions. In order to understand the As diffusion due to the thermal activation process, the diffusion coefficients of As were derived by fitting the measured SIMS depth profiles after annealing with the theoretically calculated curves. The samples employed were grown while alternatively opening and closing the As shutter to produce sharp interfaces between the doped and un-doped regions. The calculation was carried out by numerically solving the diffusion equation with the As diffusion coefficient as the fitting parameter. The SIMS depth profile before annealing was used in the calculation as a primary condition. To avoid the uniformity effect in lateral distribution of the As, for comparison the samples were cut in pairs side by side from the same wafer. It was found that the As diffusion at a lower annealing temperature of 240 °C was negligibly slow, with a diffusion coefficient of $(1.0 \pm 0.9) \times 10^{-16} \text{ cm}^2/\text{s}$. The diffusion coefficients of As of $(8 \pm 3) \times 10^{-15}$ and $(1.5 \pm 0.9) \times 10^{-13} \text{ cm}^2/\text{s}$ were obtained at 380 and 440 °C, respectively. The dependence obtained here of the As diffusion coefficient on annealing temperature is in good agreement with those previously reported on ion-implan-

ted^[13,14] or Hg-saturated LPE-grown^[15] epilayers.

To identify the effect of Hg pressure on the As diffusion, a sample was vacuum-annealed at 380 °C for 16h. It was found that the doped region was almost completely smeared out, and the corresponding diffusion coefficient was estimated to be on the order of 10^{-11} cm²/s. The enhanced diffusion of As in vacuum-annealing confirms that the As diffusion occurs via a vacancy-transfer mechanism^[15].

5 FPAs application

The MBE-grown HgCdTe were incorporated

into FPA fabrications of different formats. Figure 7 shows examples of thermal images obtained from our preliminary devices. Figure 7(a) is a scanning image obtained by a 256 × 1 LW linear FPA. The device has a back illuminated n-on-p mesa architecture with a grown-in pn heterojunction, interconnected to Si readout chips by indium bumps. Figures 7(b) and (c) are staring images of MW FPAs of 128 × 128 and 256 × 256, respectively, fabricated with planner n⁺p junctions formed by using boron implantation into a p-type HgCdTe epilayer grown on GaAs and Si.

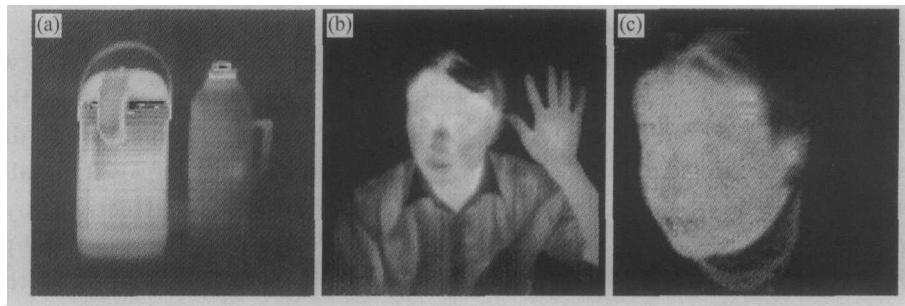


Fig. 7 Thermal images of preliminary FPA devices of LW 256 × 1 scanning (a), MW 128 × 128 (b), and MW 256 × 256 (c)

6 Conclusion

A study on MBE HgCdTe focusing on the challenging issues for the 3rd generation of IRFPAs is performed, including the growth of HgCdTe on GaAs and Si, surface defects, and p-type doping.

Improvements in compositional reproducibility were achieved. A yield of the cut-off control of 73% was obtained when screened by a maximum deviation of less than 0.2 μm from the targets. The HgCdTe epilayers showed good lateral uniformity. For a MW 75mm epilayer, the deviation in cut-off wavelength was within 0.1 μm at 80 K, satisfying the requirement for FPA fabrication.

A variety of surface defects were observed and the formation mechanism was discussed. It was found the optimal growth window was very narrow for obtaining a good morphological surface. By careful efforts in reducing substrate imperfections and controlling growth, an average surface defect density of 300 cm⁻² was obtained.

It was found that the SSC of As during

HgCdTe growth was very low and much more sensitive to the growth temperature compared to that of CdTe. The SSC was found to be only $\sim 1 \times 10^{-4}$ at 170 °C for HgCdTe. The ambient Hg played an important role in the site-transfer process during the activation anneals. The activation energy of As in HgCdTe was determined to be 19.5 meV, which decreases as $(N_a - N_d)^{1/3}$ with a slope of 3.1×10^{-5} meV · cm. The diffusion coefficient of As in HgCdTe was found to be $(1.0 \pm 0.9) \times 10^{-16}$ cm²/s, $(8 \pm 3) \times 10^{-15}$ and $(1.5 \pm 0.9) \times 10^{-13}$ cm²/s at annealing temperatures of 240, 380, and 440 °C under Hg-saturated pressure, respectively.

The MBE grown materials were incorporated into FPA fabrications of different formats. The preliminary results have been presented.

Acknowledgments The authors would like to thank the research staff and graduate students at CAMD, for they contributed tremendous research efforts and vast amounts of time to this study.

References

- [1] Donald A R, Stuart H, James C, et al. Third generation imaging sensor system concepts. SPIE, 1999, 3701: 108
- [2] Shin S H, Arias J M, Zandian M, et al. Enhanced arsenic diffusion and activation in HgCdTe. J Electron Mater, 1995, 24: 609
- [3] Zanatta J P, Ferret P, Theret G, et al. Heteroepitaxy of HgCdTe(211)B on Ge substrates by molecular beam epitaxy for infrared detectors. J Electron Mater, 1998, 27: 542
- [4] De Lyon T J, Rajavel R D, Jensen J E, et al. Heteroepitaxy of HgCdTe(112) infrared detector structures on Si(112) substrates by molecular beam epitaxy. J Electron Mater, 1996, 25: 1341
- [5] Capper P. Properties of narrow gap cadmium-based compounds. In: EMIS Datareviews Series No. 10, A5. 7. London: Inspec, 1994
- [6] Wijewarnasuriya P S, Zandian M, Young D B, et al. Microscopic defects on MBE grown LWIR HgCdTe material and their impact on device performance. J Electron Mater, 1999, 28: 649
- [7] Yang J, Wang S, Guo S, et al. Application of infrared transmission spectrum in assessment of HgCdTe epilayers. J Infrared and Millimeter Waves, 1996, 15: 327
- [8] He L, Yang J, Wang S, et al. A study of MBE growth and thermal annealing of p-type long wavelength HgCdTe. J Cryst Growth, 1997, 175/176: 677
- [9] Sivananthan S, Wijewarnasuriya P S, Aqariden F, et al. Mode of arsenic incorporation in HgCdTe grown by MBE. J Electron Mater, 1997, 26: 621
- [10] Berding M A, Sher A, Van Schilfgaarde M, et al. Modeling of arsenic activation in HgCdTe. J Electron Mater, 1998, 27: 605
- [11] Schaake H F. On the kinetics of the activation of arsenic as a p-type dopant in HgCdTe. J Electron Mater, 2001, 30: 789
- [12] Schmit J L, Bowers J E. LPE growth of $\text{Hg}_{0.60}\text{Cd}_{0.40}\text{Te}$ from Te-rich solution. J Appl Phys Lett, 1979, 35: 457
- [13] Bubulac L O, Edwall D D, Viswanathan C R. Dopant diffusion in HgCdTe grown by photon assisted molecular-beam epitaxy. J Vac Sci Technol B, 1991, 9: 1695
- [14] Myers T H, Harris K A, Yanka R W, et al. Dynamics of arsenic diffusion in metalorganic chemical vapor deposited HgCdTe on GaAs/Si substrates. J Vac Sci Technol B, 1992, 10: 1438
- [15] Chandra D, Goodwin M W, Chen M C, et al. Variation of arsenic diffusion coefficients in HgCdTe alloys with temperature and Hg pressure: Tune of p on n double layer heterojunction diode properties. J Electron Mater, 1995, 24: 599

应对第三代红外焦平面技术挑战的 HgCdTe 分子束外延

何力[†] 陈路 吴俊 巫艳 王元樟 于梅芳
杨建荣 丁瑞军 胡晓宁 李言谨 张勤耀

(中国科学院上海技术物理研究所 半导体材料器件研究中心, 上海 200083)

摘要: 叙述了围绕第三代红外焦平面的需求所进行的 HgCdTe 分子束外延的一些研究结果. 75mm HgCdTe 薄膜材料的组分均匀性良好, 80K 下截止波长偏差为 0.1 μm . 对所观察到的 HgCdTe 表面缺陷成核机制进行了分析讨论, 获得的 75mm HgCdTe 材料平均表面缺陷密度低于 300 cm^{-2} . 研究发现 As 的表面黏附系数很低, 对生长温度十分敏感, 在 170 下约为 1×10^{-4} . 计算表明, As 在 HgCdTe 中的激活能为 19.5meV, 且随 $(N_a \sum N_d)^{1/3}$ 的增大呈线性下降关系, 反比系数为 $3.1 \times 10^{-5} \text{meV} \cdot \text{cm}$. 实验发现 Hg 饱和蒸汽压下, 对应不同的温度 240, 380, 440, As 在 HgCdTe 中的扩散系数分别为 $(1.0 \pm 0.9) \times 10^{-16}$, $(8 \pm 3) \times 10^{-15}$, $(1.5 \pm 0.9) \times 10^{-13} \text{cm}^2/\text{s}$. 采用分子束外延生长的 HgCdTe 材料已用于红外焦平面探测器件的研制, 文中报道了一些初步结果.

关键词: 分子束外延; 碲镉汞; 红外焦平面

EEACC: 2520

中图分类号: TN304.54

文献标识码: A

文章编号: 0253-4177(2006)03-0381-07

[†] 通信作者. Email: lihe@mail.sitp.ac.cn

2005-08-23 收到